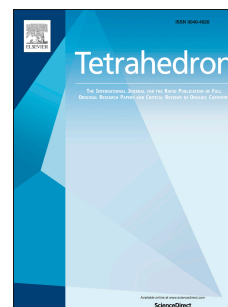


# Accepted Manuscript

A coumarin-based fluorescent and colorimetric chemosensor for rapid detection of fluoride ion

Liulei Ma, Taohua Leng, Kai Wang, Chengyun Wang, Yongjia Shen, Weihong Zhu



PII: S0040-4020(17)30057-1

DOI: [10.1016/j.tet.2017.01.034](https://doi.org/10.1016/j.tet.2017.01.034)

Reference: TET 28404

To appear in: *Tetrahedron*

Received Date: 27 November 2016

Revised Date: 12 January 2017

Accepted Date: 16 January 2017

Please cite this article as: Ma L, Leng T, Wang K, Wang C, Shen Y, Zhu W, A coumarin-based fluorescent and colorimetric chemosensor for rapid detection of fluoride ion, *Tetrahedron* (2017), doi: 10.1016/j.tet.2017.01.034.

This is a PDF file of an unedited manuscript that has been accepted for publication. As a service to our customers we are providing this early version of the manuscript. The manuscript will undergo copyediting, typesetting, and review of the resulting proof before it is published in its final form. Please note that during the production process errors may be discovered which could affect the content, and all legal disclaimers that apply to the journal pertain.

## Graphical Abstract

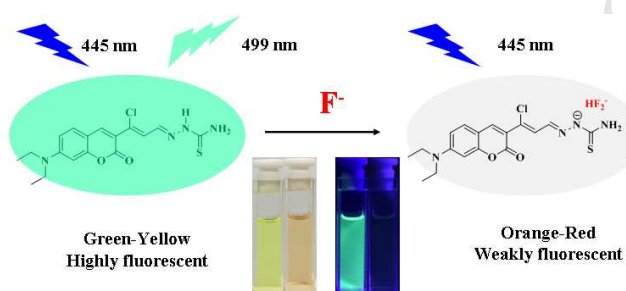
**A coumarin-based fluorescent and colorimetric **chemosensor** for rapid detection of fluoride ion**

Liulei Ma<sup>a</sup>, Taohua Leng<sup>b</sup>, Kai Wang<sup>a</sup>,  
Chengyun Wang<sup>a,\*</sup>, Yongjia Shen<sup>a</sup>, Weihong  
Zhu<sup>a,\*</sup>

<sup>a</sup>Key Laboratory for Advanced Materials and Institute of Fine Chemicals, School of Chemistry and Molecular Engineering, East China University of Science & Technology, Shanghai 200237, P. R. China.

<sup>b</sup>National Food Quality Supervision and Inspection Center (Shanghai) / Shanghai Institute of Quality Inspection and Technical Research, Shanghai 200233, P. R. China.

A colorimetric and fluorescent sensor for the detection of fluoride anion has been designed and synthesized. The sensor showed evident naked-eye color variation from green-yellow to orange-red after treatment with F<sup>-</sup>, and its fluorescence was effectively quenched within 3 seconds.





Tetrahedron

journal homepage: www.elsevier.com



# A coumarin-based fluorescent and colorimetric chemosensor for rapid detection of fluoride ion

Liulei Ma<sup>a</sup>, Taohua Leng<sup>b</sup>, Kai Wang<sup>a</sup>, Chengyun Wang<sup>a,\*</sup>, Yongjia Shen<sup>a</sup>, Weihong Zhu<sup>a,\*</sup>

<sup>a</sup> Key Laboratory for Advanced Materials and Institute of Fine Chemicals, School of Chemistry and Molecular Engineering, East China University of Science & Technology, Shanghai 200237, P. R. China.

<sup>b</sup> National Food Quality Supervision and Inspection Center (Shanghai) / Shanghai Institute of Quality Inspection and Technical Research, Shanghai 200233, P. R. China.

## ARTICLE INFO

### Article history:

Received

Received in revised form

Accepted

Available online

### Keywords:

Coumarin

Thiosemicarbazone

Fluorescent probe

Fluoride anion

## ABSTRACT

A novel coumarin-based compound **1** featuring thiosemicarbazone as binding unit, was reported as a colorimetric and fluorescent probe for the detection of fluoride anion. The addition of F<sup>-</sup> to a solution of probe **1** in tetrahydrofuran resulted in evident naked-eye color change from green-yellow to orange-red under daylight and obvious fluorescence quenching within 3 seconds. And the detection limit toward F<sup>-</sup> was calculated to be as low as  $2.16 \times 10^{-7}$  mol/L. <sup>1</sup>H NMR titrations proved that the interaction between **1** and fluoride ion: hydrogen bond at low fluoride ion concentration, deprotonation at high fluoride ion concentration. Besides, it exhibited highly sensitivity and selectivity for F<sup>-</sup> over other examined ions (Cl<sup>-</sup>, Br<sup>-</sup>, I<sup>-</sup>, AcO<sup>-</sup>, NO<sub>3</sub><sup>-</sup>, HSO<sub>4</sub><sup>-</sup>, H<sub>2</sub>PO<sub>4</sub><sup>-</sup>) in tetrahydrofuran solution.

2016 Elsevier Ltd. All rights reserved.

## 1. Introduction

The recognition and sensing of anions has been a key research theme because of the fundamental and crucial roles of anions in biological and environmental fields.<sup>1-5</sup> Among the entire range of biologically anions, fluoride anion possesses significant potential in the prevention of dental caries and treatment for osteoporosis.<sup>6,7</sup> However, excess intake fluoride can cause many serious diseases such as fluorosis, acute stomach and kidney problems.<sup>8-9</sup> Besides, fluoride ion is one of the most attractive targets owing to its smallest ionic radius, highest charge density and hard Lewis basic nature.<sup>10-12</sup> Thus, simple and efficient detection of F<sup>-</sup> with high selectivity and sensitivity is in great need.

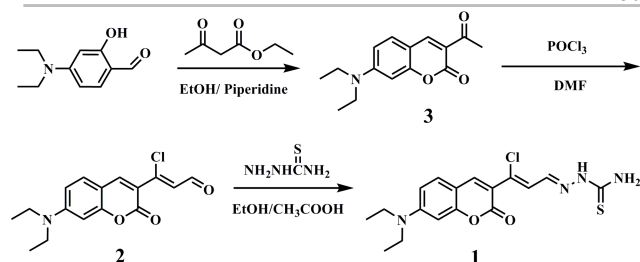
So far fluoride-detecting and-sensing techniques can be classified into several kinds, such as (a) the electrode method;<sup>13</sup> (b) <sup>19</sup>F NMR analysis;<sup>14</sup> (c) fluorescent or colorimetric sensing. Compared with other detecting methods, colorimetric and fluorescent chemosensors have been recognized as a promising and powerful tool for sensing fluoride ion owing to its advantages of high selectivity, sensitivity and practical operation.<sup>15-18</sup> Recently, Molecules containing thiosemicarbazone were used to detect fluoride anion. Su<sup>19</sup> et al. reported two thioxanthone-based F<sup>-</sup> sensors, in which thiosemicarbazone acted as responding unit, their work offer the possibility and

convenience for the multiple detection of Hg<sup>2+</sup> and F<sup>-</sup>. Jiang<sup>20</sup> et al. reported a simple and efficient chemosensor, 2-(naphthylmethylene) hydrazinecarbothioamide, which showed high selectivity and sensitivity toward fluoride anion in both absorption and fluorescence modes. For this kind of sensors, N-H deprotonation, or hydrogen-bond-induced  $\pi$ -electron delocalization, are believed to be responsible for signaling the binding event.<sup>21-23</sup>

With this in mind, compound **1**, 3-chloro-3-(7-(diethylamino)-2-oxo-2H-chromen-3-yl)allylidene-hydrazine-carbothioamide, in which substituted coumarin acted as signalling unit and thiosemicarbazone acted as responding unit, was rationally designed and synthesized. Compared with conventional coumarin dyes, both 7-diethylamino and imine units in **1** extended the conjugate structure of the fluorophore. As expected, probe **1** showed strong emission at 499 nm in THF with a fluorescent quantum yield of 0.34. Furthermore, the fluorescence turn-off sensor showed high selectivity for fluoride ion through the deprotonation action and the photo-induced electron transfer (PET) mechanism. More importantly, probe **1** could detect fluoride anion by a fast method which was observable with naked eyes. And it showed a faster response (within 3s) to fluoride ion than that of some related literatures.<sup>24-26</sup>

## 2. Results and discussion

\* Corresponding author: Tel/fax: +086-21-64252967; E-mail address: cywang@ecust.edu.cn (C.-Y. Wang), whzhu@ecust.edu.cn (W.-H. Zhu)



Scheme 1. Synthetic route of compound 1

### 2.1 Synthesis

Compound **1** was synthesized according to the route in Scheme 1. The intermediate **2** and final product **1** were confirmed by  $^1\text{H}$  NMR,  $^{13}\text{C}$  NMR, and HRMS spectra (Electronic Supporting Information (ESI), Fig.S1-S6).

### 2.2. Spectral properties of compound 1

The interactions between compound **1** and various anions ( $\text{F}^-$ ,  $\text{Cl}^-$ ,  $\text{Br}^-$ ,  $\text{I}^-$ ,  $\text{AcO}^-$ ,  $\text{NO}_3^-$ ,  $\text{HSO}_4^-$ ,  $\text{H}_2\text{PO}_4^-$ ) were investigated in THF solution through colorimetric and fluorescent analysis. When probe **1** was treated with  $\text{F}^-$ , the system changed from green-yellow to orange-red within 3s, while other anions did not show prominent visible color changes (Fig. 1a). Besides, under 365 nm UV lamp, the color of the system changed from light green to dark, only responding to  $\text{F}^-$  among eight anions (Fig. 1b).

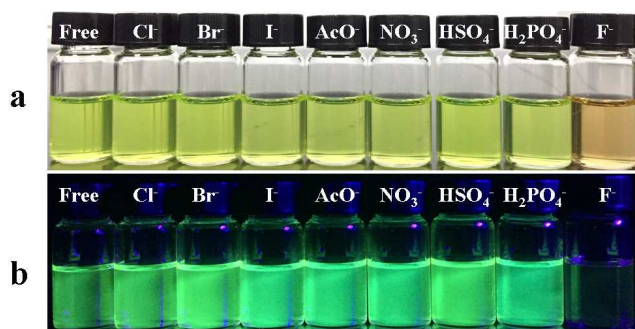


Fig. 1 Color changes of **1** ( $1.0 \times 10^{-5}$  M) towards 10 equiv of various anions in THF under daylight (a) and 365 nm UV lamp (b).

In order to deduce the anion sensing ability of compound **1**, titrations were carried out in THF solution and were monitored by UV-visible spectroscopy. The experiment was performed by preparing a solution ( $1 \times 10^{-5}$  mol/L) of the sensor in THF and followed by the addition of tetrabutylammonium fluoride (TBAF) solution (0.02 mol/L). Fig. 2a displayed the UV-vis absorption titrations of the compound **1** with various amount of fluoride ion in THF at  $20^\circ\text{C}$ . The molar extinction coefficient of **1** (445 nm) was  $7.08 \times 10^4$  L/(mol cm) by calculation. Upon treatment with  $\text{F}^-$ , the main absorption band at 445 nm of **1** gradually decreased with concomitant formation of a long wavelength absorption band centered at 510 nm (4-10 equiv), and with an isosbestic point at around 480 nm. Correspondingly, the absorption red-shift of 65 nm resulted in the solution distinct color change, which can be directly observed by naked eyes. Besides, the absorption peak at 445 nm and 510 nm reached equilibrium upon adding 10 equiv of fluoride ion (Fig. S7).

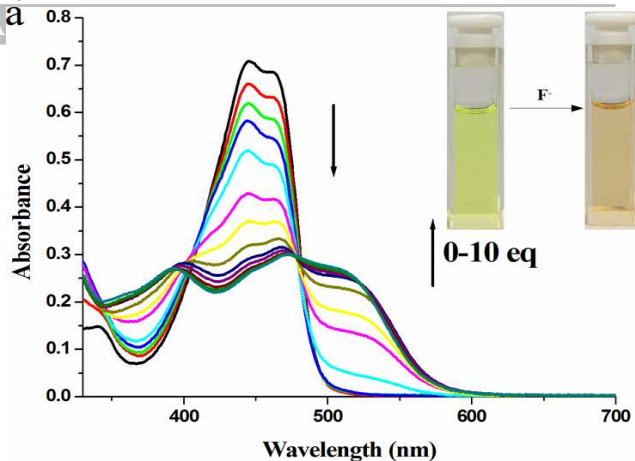


Fig. 2a UV-vis absorption spectra of **1** ( $1 \times 10^{-5}$  M) in the presence of TBAF in THF. Inset: color change of **1** upon addition of  $\text{F}^-$  (100  $\mu\text{M}$ ) under daylight.

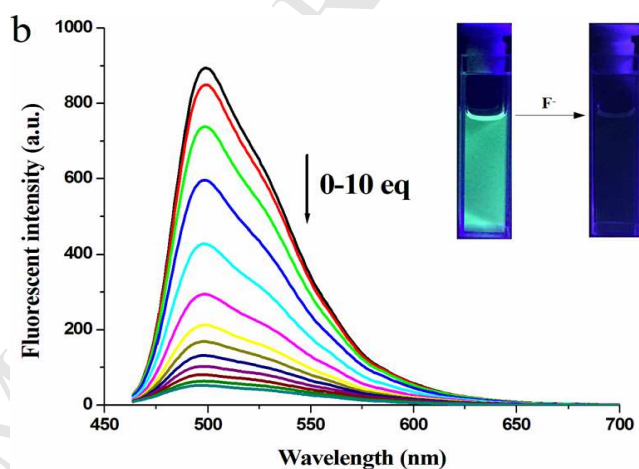


Fig. 2b The fluorescent spectra of **1** ( $1 \times 10^{-5}$  M) in the presence of TBAF in THF. Inset: color change of **1** upon addition of  $\text{F}^-$  (100  $\mu\text{M}$ ) under 365 nm light. ( $\lambda_{\text{ex}} = 445$  nm)

The fluorescence responses of **1** toward various amount of fluoride ion were also performed in THF at  $20^\circ\text{C}$ . As shown in Fig. 2b and Fig. S8, upon the addition of  $\text{F}^-$ , the fluorescence intensity of **1** at 499 nm was almost linearly decreased and 91% of the fluorescence intensity was quenched by calculation upon addition of 10 equiv of fluoride ion.

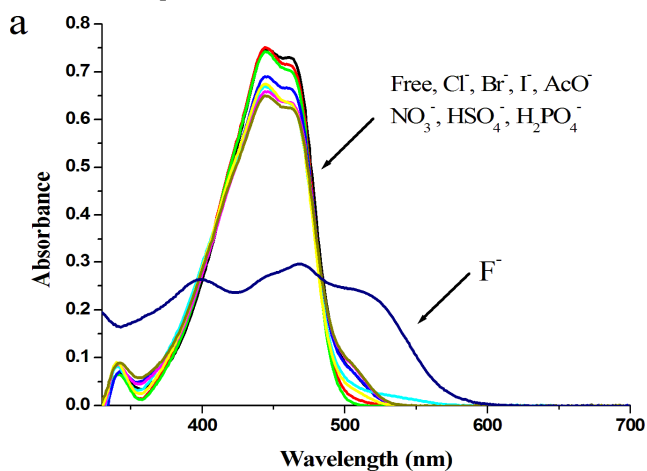
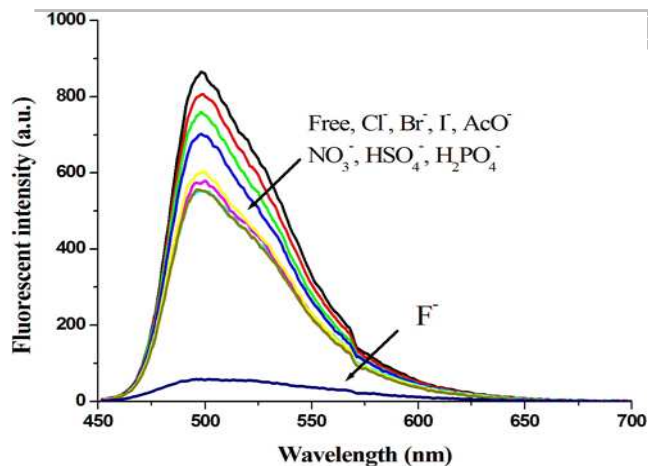


Fig. 3a Absorption spectra of **1** ( $1.0 \times 10^{-5}$  M) in the presence of  $\text{F}^-$  (10 equiv),  $\text{Cl}^-$ ,  $\text{Br}^-$ ,  $\text{I}^-$ ,  $\text{AcO}^-$ ,  $\text{NO}_3^-$ ,  $\text{HSO}_4^-$ ,  $\text{H}_2\text{PO}_4^-$  (20 equiv, respectively).



**Fig. 3b** Fluorescent spectra of **1** ( $1.0 \times 10^{-5}$  M) in the presence of  $F^-$  (10 equiv),  $Cl^-$ ,  $Br^-$ ,  $I^-$ ,  $AcO^-$ ,  $NO_3^-$ ,  $HSO_4^-$ ,  $H_2PO_4^-$  (20 equiv, respectively).

The interference of other anions to the detection of  $F^-$  were also investigated to test the sensing selectivity, and the experimental results suggested that sensor **1** showed high selectivity for the fluoride anion in colorimetric and fluorometric modes. As depicted in Figs. 3a and 3b, neither prominent absorption nor fluorescence changes were found with excess addition of other halide ions ( $Cl^-$ ,  $Br^-$ ,  $I^-$ ) as well as  $AcO^-$ ,  $NO_3^-$ ,  $HSO_4^-$ ,  $H_2PO_4^-$ . It means probe **1** showed specific sensitivity and selectivity for  $F^-$  over other examined ions in tetrahydrofuran solution.

### 2.3 Calculation of detection limit

The detection limit was calculated on the basis of fluorescence titrations. A plot of fluorescence intensity change of **1** ( $10.0 \mu M$ ) against varied concentrations of  $F^-$  ( $10.0$ – $60.0 \mu M$ ) in THF ( $\lambda_{ex} = 445$  nm, slit: 5 nm/5 nm, PMT Volts: 550V.).  $R^2 = 0.9924$ ,  $k = 1.34 \times 10^7$  au/M. The Standard deviation ( $\sigma = 0.9656$ ) was obtained by fluorescence responses (5-times of consecutive scanning on the Varian Cary Eclipse Fluorescence Spectrophotometer). Therefore, the detection limit was calculated by the formula:

$$\text{Detection limit} = 3\sigma/k = 2.16 \times 10^{-7} M$$

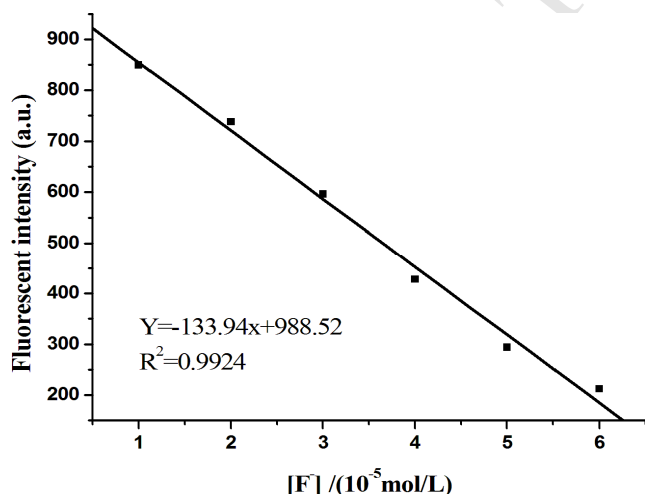


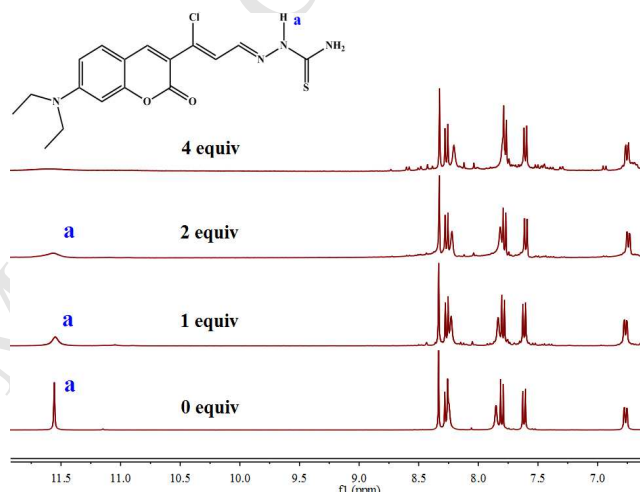
**Fig. 4** The fluorescent intensity of **1** at 499 nm in different concentration of fluoride. ( $\lambda_{ex} = 445$  nm)

### 2.4 $^1H$ NMR titration experiments

To get insight into the interaction between receptor **1** and  $F^-$ ,  $^1H$  NMR titration experiments were carried out in  $DMSO-d_6$  solution with different amount of  $F^-$  anion (0, 1, 2 and 4 equiv).

As shown in Fig. 5, upon addition of 1 equiv of  $F^-$ , the signal peak of N-H active proton at 11.55 ppm broadened and decreased. Upon addition of 2 equiv of  $F^-$ , the resonance signal corresponding to the N-H proton showed severe broadening, this result suggested that hydrogen-bond interaction existed between target compound and TBAF at low fluoride ion concentration. Upon addition of 4 equiv of  $F^-$ , the resonance signal of the N-H proton disappeared and the result suggested that compound **1** would be deprotonated at higher fluoride ion concentration. Meanwhile, the chemical shifted values of N-H active proton and aromatic protons remained unaltered. These observations indicated that the deprotonation process of thiourea N-H segment is involved in the receptor's interaction with fluoride anion to increase the electron density on the N atom, associated with enhancement in the electron transfer effect of the PET (Photo-induced Electron Transfer) transition. The color changed from light green to dark under 365 nm UV lamp is visible evidence for this.

Hence, the result of  $^1H$  NMR titrations provided a supporting proof for the following proposed detection mechanism between receptor **1** and  $F^-$ .



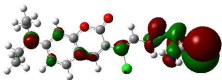
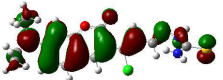
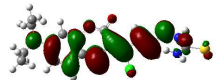
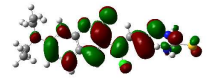


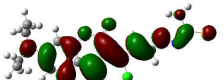
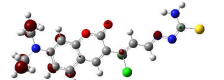
**Fig. 5**  $^1H$  NMR titration spectra of **1** in  $DMSO-d_6$  in the presence of various equivalents of TBAF.

### 2.5 Theoretical calculations

To further understand the sensing mechanism, theoretical calculations were performed for **1**, and **1**+ $F^-$  (deprotected product) by using the Gaussian 09 package at the B3LYP level of theory<sup>27</sup> (Tables 1 and 2). The calculated results revealed that the highest occupied molecular orbital (HOMO) (-6.775 eV) and lowest unoccupied molecular orbital (LUMO) (-1.946 eV) of **1** were both located at the units of coumarin and thiosemicarbazone. The DFT calculations revealed that the energy singlet transition of HOMO-LUMO characterized with an energy gap of 4.829 eV. According to the fluorescence emission mechanism, the excited electron of the coumarin unit of **1** is back to the ground state and radiates strong fluorescence.

When **1**+ $F^-$  was generated after adding fluoride ion, the LUMO (-1.193 eV) was mainly located at the unit of coumarin, the HOMO (-5.614 eV) was more distributed on the thiosemicarbazone unit and slight distribution of coumarin unit. Additionally, the difference in energy gap between HOMO and LUMO of sensor **1**+ $F^-$  was calculated to be 4.421 eV. As the frontier molecular orbitals are spreading over thiosemicarbazone and coumarin unit, the excited electron of thiosemicarbazone unit is back to the ground state of coumarin unit and therefore leads the quenching of the fluorescence. Besides, the decrease of energy gap ( $4.829 \text{ eV} \rightarrow 4.421 \text{ eV}$ ) can interpret that the red-shift

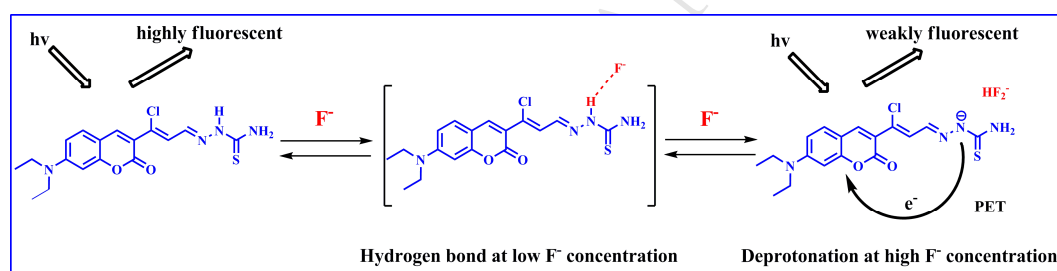
**Table 1.** Calculated surfaces of HOMO-1, HOMO, LUMO, and LUMO+1 (1, 1+F<sup>-</sup>).

	HOMO-1	HOMO	LUMO	LUMO+1
1				
1+F <sup>-</sup>				

**Table 2.** Calculated energy of HOMO-1, HOMO, LUMO, and LUMO+1(1, 1+F<sup>-</sup>).

	HOMO-1(eV)	HOMO(eV)	LUMO(eV)	LUMO+1(eV)	HOMO-LUMO(eV)	HOMO-(LUMO+1) (eV)
1	-7.523	-6.775	-1.946	-0.599	4.829	6.176
1+F <sup>-</sup>	-6.420	-5.614	-1.193	-0.008	4.421	5.606

## 2.6 Detection mechanism

**Fig. 6** Proposed sensing mechanism

Combining the theoretical calculations with the <sup>1</sup>H NMR titration experiments, we deduce that F<sup>-</sup> interacts with **1** through hydrogen bonding at lower concentrations, but at higher concentrations it induces the deprotonation of the N-H proton. After deprotonation, the electron transfer effect of the PET transition would be enhanced due to the increase of the electron density on the nitrogen, which leads the quenching of the fluorescence. The proposed detection mechanism is vividly described in Fig. 6.

## 3. Conclusions

In this paper, a novel coumarin-based imine, compound **1**, was designed, synthesized and characterized. The colorimetric and fluorescent sensor performed high selectivity, short response time and excellent sensitivity toward F<sup>-</sup> over other anions (Cl<sup>-</sup>, Br<sup>-</sup>, I<sup>-</sup>, AcO<sup>-</sup>, NO<sub>3</sub><sup>-</sup>, HSO<sub>4</sub><sup>-</sup>, H<sub>2</sub>PO<sub>4</sub><sup>-</sup>) in THF solution with low detection limit of 2.16×10<sup>-7</sup> M and high fluorescence quantum yield of 0.34. Upon treatment with F<sup>-</sup>, the color change (light green→dark) was observed under 365 nm light, which was attributed to the enhancement in the electron transfer effect of the PET process through the deprotonation of N-H active proton. All above-mentioned facts suggested probe **1** potentially provided an alternative and simple approach for detecting trace amount of F<sup>-</sup>.

## 4. Experimental

### 4.1 Materials and measurements

THF was distilled under argon atmosphere from sodium and benzophenone immediately prior to use. Unless otherwise stated, all reagents and solvents were AR grade purchased from commercial suppliers and used without further purification. <sup>1</sup>H NMR and <sup>13</sup>C NMR spectra were measured on a Bruker AM-400 spectrometer at room temperature using *d*-chloroform or DMSO-*d*<sub>6</sub> as a solvent and tetramethylsilane (TMS, δ=0 ppm) as an internal standard. High resolution mass spectra (HRMS) were obtained by a Waters LCT Premier XE spectrometer. The UV/Vis spectra were recorded on a Nicolet CARY 100 and the Fluorescence spectra were measured on a Varian CARY Eclipse (1 cm quartz cell).

The stock solution of **1** (1×10<sup>-5</sup> mol/L) was prepared in THF solution. The TBA salts (F<sup>-</sup>, Cl<sup>-</sup>, Br<sup>-</sup>, I<sup>-</sup>, AcO<sup>-</sup>, NO<sub>3</sub><sup>-</sup>, HSO<sub>4</sub><sup>-</sup> and H<sub>2</sub>PO<sub>4</sub><sup>-</sup>) solutions were also prepared at the concentration of 2×10<sup>-2</sup> mol/L in THF. Different equivalents of TBA salts were added to the probe solution and their corresponding UV-visible and fluorescence spectra were recorded at 20 °C. Compound **1** (5×10<sup>-3</sup> mol/L) was titrated with fluoride anion (as tetrabutylammonium salts) by addition of increasing equivalents of F<sup>-</sup> in DMSO-*d*<sub>6</sub>.

## 3-acetyl-7-diethylamino-2H-chromen-2-one (3)

The intermediate **3** was synthesized according to the literature<sup>28</sup> with a minor modification. 4-*N,N*-Diethylamino-salicylaldehyde (1.93 g, 10 mmol), ethyl acetoacetate (1.95 g, 15 mmol), and 3 drops of piperidine were dissolved in 20 mL of absolute ethanol. After the mixture solution was refluxed for 8 h, the solvent was removed under reduced pressure. The yellow solid was precipitated and collected, and the crude product was recrystallized from absolute ethanol to afford compound **3** (2.0 g, 77%). <sup>1</sup>H NMR (400 MHz, CDCl<sub>3</sub>, TMS) δ: 8.42-8.41 (d, 1H, J=2.2 Hz), 7.39-7.37 (m, 1H), 6.62-6.59 (m, 1H), 6.46-6.45 (d, 1H, J=2.4 Hz), 3.47-3.42 (q, 4H, J=7.2 Hz), 2.67 (t, 3H, J=7.2 Hz), 1.25-1.21 (t, 6H, J=7.2 Hz).

## 3-chloro-3-(7-(diethylamino)-2-oxo-2H-chromen-3-yl) acylaldehyde (2)

The intermediate **2** was synthesized according to the reported method<sup>29-30</sup> with a minor modification. In a 100mL three-necked round bottomed flask, *N,N*-dimethyl formamide (10.0 mL) and compound **3** (2.6 g, 10.0 mmol), were taken and cooled to 0-5 °C with stirring under Ar. To the above solution phosphorous oxychloride (4.45 g, 2.70 mL, 27.0 mmol) was added dropwise maintaining the temperature of the reaction mass at 0-5 °C. The reaction mixture was stirred at 0-5 °C for 3 h, then allowed to attain room temperature and then heated at 80-85 °C for 8 h. Subsequently, the reaction mass was cooled to room temperature and poured in to crushed ice with stirring and deep external cooling, the clear solution was neutralized with sodium carbonate to pH 7-8, by keeping the temperature below 10 °C. The product was filtered, washed with ice cold water and dried. The compound **2** was crystallized from ethanol as brick red power (2.0 g, 65%). <sup>1</sup>H NMR (400 MHz, CDCl<sub>3</sub>, TMS) δ: 10.27 (d, 1H, J=6.8 Hz), 8.37 (s, 1H), 7.67 (d, 1H, J=6.8 Hz), 7.40 (d, 1H, J=8.8 Hz), 6.66-6.63 (dd, 1H, J=8.8 Hz, 8.8Hz), 6.48 (d, 1H, J=2.4 Hz), 3.50-3.44 (q, 4H, J=6.8 Hz), 1.27-1.23 (t, 6H, J=6.8 Hz); <sup>13</sup>C NMR (100 MHz, CDCl<sub>3</sub>, TMS) δ: 192.35, 158.39, 156.78, 152.66, 145.22, 144.82, 131.01, 126.17, 112.94, 109.93, 108.38, 96.49, 45.19, 12.47. HRMS (ESI) calcd for C<sub>16</sub>H<sub>16</sub>ClNO<sub>3</sub> MH<sup>+</sup> 328.0716, found 328.0714.

## 3-chloro-3-(7-(diethylamino)-2-oxo-2H-chromen-3-yl)allylidenehydrazinecarbothioamide (1)

Compound **2** (0.305 g, 1 mmol), thiosemicarbazide (0.091 g, 1 mmol), and 20 mL of ethanol were added to 100 mL round-bottom flask, and then 5 drops of CH<sub>3</sub>COOH was added to the system. The reaction mixture was stirred at 80 °C for 8 h. The precipitate was filtered after the final reaction mixture was cooled to room temperature. The precipitate was washed repeatedly with ethanol and dried under vacuum to obtain orange compound **1** (0.20 g, 82%). MP: 226-228°C. <sup>1</sup>H NMR (400 MHz, DMSO-*d*<sub>6</sub>, TMS) δ: 11.56 (s, 1H), 8.34 (s, 1H), 8.28 (d, 1H, J=9.2 Hz), 8.26 (s, 1H), 7.86 (s, 1H), 7.81 (d, 1H, J=9.2 Hz), 7.63 (d, 1H, J=9.2 Hz), 6.75 (dd, 1H, J=8.8 Hz, 9.2Hz), 6.56 (d, 1H, J=2.0Hz), 3.49-3.44 (q, 4H, J=6.8 Hz), 1.16-1.12 (t, 6H, J=6.8 Hz); <sup>13</sup>C NMR (100 MHz, DMSO-*d*<sub>6</sub>, TMS) δ: 177.66, 158.22, 155.39, 151.70, 142.25, 141.49, 132.32, 130.84, 124.35, 113.12, 109.87, 107.76, 95.68, 44.27, 12.28. HRMS (ESI) calcd for C<sub>17</sub>H<sub>19</sub>ClN<sub>4</sub>O<sub>2</sub>S MH<sup>+</sup> 379.0996, found 379.0999.

## Acknowledgements

We gratefully acknowledge the financial support by the Natural Science Foundation of Shanghai (16ZR1408000), and the National Key Program of China (2016YFA0200302).

<sup>1</sup>H NMR, <sup>13</sup>C NMR and HRMS spectra of the intermediate **2** and final product **1** are available. Additional UV-vis absorption and emission spectra related to this article can be found in ESI.

## References and notes

- Du, J. J.; Hu, M. M.; Fan, J. L.; Peng, X. J. *Chem. Soc. Rev.* **2012**, 41, 4511-4535.
- Ashton, T. D.; Jolliffe, K. A.; Pfeffer, F. M. *Chem. Soc. Rev.* **2015**, 44, 4547-4595.
- Lee, M. H.; Kim J. S.; Sessler, J. L. *Chem. Soc. Rev.* **2015**, 44, 4185-4191.
- Ren, J.; Wu, Z.; Zhou, Y.; Li, Y.; Xu, Z. X. *Dyes Pigm.* **2011**, 91, 442-445.
- Ke, B. W.; Chen, W. X.; Ni, N. T.; Cheng, Y. F.; Dai, C. F.; Dinh, H.; Wang, B. H. *Chem. Commun.* **2013**, 49, 2494-2496.
- Amalraj, A.; Pius, A. J. *Fluorine Chem.* **2015**, 178, 73-78.
- Bao, Y. Y.; Liu, B.; Wang, H.; Tian, J.; Bai, R. K. *Chem. Commun.* **2011**, 47, 3957-3959.
- Zhang, L.; Wang, L. M.; Zhang, G. J.; Yu, J. J.; Cai, X. F.; Teng, M. S.; Wu, Y. *Chin. J. Chem.* **2012**, 30, 2823-2826.
- Xiong, J.; Sun, L.; Liao, Y.; Li, G. N.; Zuo, J. L.; You, X. Z. *Tetrahedron Lett.* **2011**, 52, 6157-6161.
- Zhang, J. F.; Zhou, Y.; Yoon, J.; Kim, J. S. *Chem. Soc. Rev.* **2011**, 40, 3416-3429.
- Cao, X. W.; Lin, W. Y.; Yu, Q. X.; Wang, J. L. *Org. Lett.* **2011**, 13, 6098-6101.
- Yu, M. M.; Xu, J.; Peng, C.; Li, Z. X.; Liu, C. X.; Wei, L. H. *Tetrahedron.* **2016**, 72, 273-278.
- Cosentino, P.; Grossman, B.; Shieh, C.; Doi, S.; Xi, H.; Erbland, P. J. *Geotech. Eng.* **1995**, 121, 610-617.
- Konieczka, P.; Zygmunt, B.; Namiesnik, J. *Bull. Environ. Contam. Toxicol.* **2000**, 64, 794-803.
- Zhou, Y.; Zhang, J. F.; Yoon, J. *Chem. Rev.* **2014**, 114, 5511-5571.
- Gai, L. Z.; Mack, J.; Lu, H.; Nyokong, T.; Li, Z. F.; Kobayashi, N.; Shen, Z. *Coord. Chem. Rev.* **2015**, 285, 24-51.
- Hu, J. Y.; Liu, R.; Cai, X.; Shu, M. L.; Zhu, H. J. *Tetrahedron.* **2015**, 71, 3838-3843.
- Wang, J. B.; Zong, Q. S.; Wu, Q. Q.; Shen, J. J.; Dai, F. Y.; Wu, C. J. *Tetrahedron.* **2015**, 71, 9611-9616.
- Ding, L.; Wu, M. J.; Li, Y. R.; Chen, Y.; Su, J. H. *Tetrahedron Lett.* **2014**, 55, 4711-4715.
- Lu, W.; Zhang, M. Y.; Liu, K. Y.; Fan, B.; Xia, Z.; Jiang, L. M. *Sens. Actuators B.* **2011**, 160, 1005-1010.
- Sharma, S.; Hundal, M. S.; Hundal, G. *Tetrahedron Lett.* **2013**, 54, 2423-2427.
- Peng, X. J.; Wu, Y. K.; Fan, J. L.; Tian, M. Z.; Han, K. L. *J. Org. Chem.* **2005**, 70, 10524-10531.
- De Silva, A. P.; Moody, T. S.; Wright, G. D. *Analyst.* **2009**, 134, 2385-2393.
- Wang, C. Y.; Yang, S.; Yi, M.; Liu, C. H.; Wang, Y. J.; Li, J. S.; Li, Y. H.; Yang, R. H. *Appl. Mater. Interfaces.* **2014**, 6, 9768-9775.
- Zhou, X. Q.; Lai, R.; Li, H.; Stains, C. I. *Anal. Chem.* **2015**, 87, 4081-4086.
- Tan, W. B.; Leng, T. H.; Lai, G. Q.; Li, Z. F.; Wu, J. F.; Shen, Y. J.; Wang, C. Y. *Chin. J. Chem.* **2016**, 34, 809-813.
- Wu, J. F.; Lai, G. Q.; Li, Z. F.; Lu, Y. X.; Leng, T. H.; Shen, Y. J.; Wang, C. Y. *Dyes Pigm.* **2016**, 124, 268-276.
- Wu, J. S.; Sheng, R. L.; Liu, W. M.; Wang, P. F.; Zhang, H. Y.; Ma, J. J. *Tetrahedron.* **2012**, 68, 5458-5463.
- Debnath, T.; Dana, J.; Maity, P.; Lobo, H.; Shankarling, G. S.; Ghosh, H. N. *Chem. Eur. J.* **2015**, 21, 5704-5708.
- Debnath, T.; Dana, J.; Maity, P.; Lobo, H.; Singh, B.; Shankarling, G. S.; Ghosh, H. N. *Chem. Eur. J.* **2014**, 20, 3510-3519.